

THIS IS A PREPRINT --- SUBJECT TO CORRECTION

Determination of Laminar, Turbulent, and Transitional Foam Flow Losses in Pipes

By

R.E. Blauer, B.J. Mitchell, and C.A. Kohlhaas, Members SPE-AIME,
Colorado School of Mines

©Copyright 1974

American Institute of Mining, Metallurgical, and Petroleum Engineers, Inc.

This paper was prepared for the 44th Annual California Regional Meeting of the Society of Petroleum Engineers of AIME, to be held in San Francisco, Calif., April 4-5, 1974. Permission to copy is restricted to an abstract of not more than 300 words. Illustrations may not be copied. The abstract should contain conspicuous acknowledgment of where and by whom the paper is presented. Publication elsewhere after publication in the JOURNAL OF PETROLEUM TECHNOLOGY or the SOCIETY OF PETROLEUM ENGINEERS JOURNAL is usually granted upon request to the Editor of the appropriate journal provided agreement to give proper credit is made.

Discussion of this paper is invited. Three copies of any discussion should be sent to the Society of Petroleum Engineers office. Such discussion may be presented at the above meeting and, with the paper, may be considered for publication in one of the two SPE magazines.

ABSTRACT

In arriving at a method for predicting friction losses in laminar, transitional, and turbulent flow regimes for flowing foam, it was found Reynold's numbers and Fanning friction factors could be calculated with effective foam viscosity, actual foam density, average velocity, and true pipe diameter. Further, it was found the relationship between Reynold's number and Fanning friction factor for foam was identical to that of single-phase fluids. The test data were taken under controlled flow in capillary tubes and 1-1/4-inch and 2-3/8-inch oilfield seamless tubing. Friction losses of foam within 2-7/8-inch tubing and 4-1/2-inch and 5-1/2-inch casing during fracture treatments have been accurately predicted using the proposed method.

INTRODUCTION

Foam has been used for several years as a wellbore clean-out and drilling fluid and to a very limited extent as a fluid loss, diverting, and fracturing fluid. Applications have been limited because the behavior of the foam could not be confidently predicted. Major problems when using
References and illustrations at end of paper.

foam in oilwell treatments were the calculation of friction loss, wellhead pressure, and the resulting density and carrying capacities during treatment.

Lockhart and Martinelli,¹ developed the most popular empirical correlation for predicting friction losses of flowing two-phase fluids within horizontal pipes. This method was sufficiently accurate only for pressure losses within pipes smaller than 2-inches in diameter.² Other empirical correlations^{3, 4, 5} based on mechanical energy or momentum losses proved insufficient also.

Bertuzzi, Tek, and Poettmann's⁶ energy dissipation function which has extensive oilfield use for predicting pressure losses within horizontal pipes for non-uniformly mixed, two-phase fluids was found not reliable for foam.

Failures of these empirical two-phase correlations for the prediction of pressure losses for foam flow may be lodged in the theoretical developments by Einstein⁷ and Hatschek^{8, 9}. They point out foam should be treated as a single-phase fluid with viscosities significantly greater than either phase. Mitchell¹⁰ used these theories to experimentally find viscosities of foam.

He¹¹ also showed foam approximately exhibits Bingham plastic behavior and presented plastic viscosities and yield strength data.

Krug and Mitchell's¹² modifications in existing single-phase fluid-flow equations account for both the compressibility of the gas within the foam and the resulting changes in the viscosity. The resultant equations were applicable to the circulation of foam within a wellbore; however, these equations were limited to laminar flow and lacked empirical justification.

The foregoing theories and empiricism and additional field and laboratory work have been combined to devise a method for predicting the type of regime in which the foam is flowing and a method for calculating the pressure losses of foam flowing within horizontal or vertical pipes.

EFFECTIVE VISCOSITY OF FOAM

Foam in this study is a homogeneous mixture of air or nitrogen, fresh water, and a surface-active agent. The gas phase exists as microscopic gas-bubbles suspended in the water and surfactant solution. In practice these bubbles may occupy between 10 and 95 percent of the total foam volume.

Foam quality is the ratio of gas volume to the total foam volume.

$$\Gamma_{T,P} = \frac{V_{sg}}{V_f} \dots \dots \dots (1)$$

Since the gas is compressible, temperature and pressure of the foam must be specified.

Figure 1 was developed from the theories of Einstein and Hatschek and laboratory measurements by Mitchell. Three separate theories, each with a physical model dependent on quality, were required to fully determine and understand foam viscosity.

The spherical gas-bubbles in foams with qualities between 0.00 and 0.52 are uniformly dispersed in the liquid and do not contact other bubbles. Flow is Newtonian. At 0.52 quality the spherical bubbles are packed loosely in a cubic arrangement and begin to interfere by contacting each other during flow. Above 0.74 quality the

bubbles are no longer spheres and deform to parallelepipeds during flow.

Einstein's theory is valid for foam qualities less than 0.52. The derivation of his two-phase viscosity is based on an energy balance and the following assumptions;

1. Solid spherical particles are suspended in a homogeneous fluid.
2. All particles are homogeneous, weightless, and have identical volumes and diameters.
3. Spacing of the particles is uniform and the particles do not touch.
4. There is no slip at the surface of the particles.

Einstein's equation for the viscosity of foam is

$$\mu_f = \mu_l (1.0 + 2.5 \Gamma_{T,P}) \dots \dots (2)$$

Hatschek's theories explain foam viscosity for the bubble-interference and bubble-deformation quality ranges. The interference between the spherical bubbles in foams with qualities between 0.52 and 0.74 requires additional work be applied to initiate and maintain flow. This additional work accounts for high foam apparent viscosity. Hatschek's viscosity for bubble-interference foam is

$$\mu_f = \mu_l (1.0 + 4.5 \Gamma_{T,P}) \dots \dots (3)$$

His next argument was the deformation of the bubbles within foams which have qualities above 0.74 causes the geometric shape of the bubbles to proceed from spheres to dodecahedra and finally to parallelepipeds, and this bubble configuration is the only one which can flow in laminae. The viscosity of the foam caused by the shear of the fluid between the parallelepiped gas bubbles is

$$\mu_f = \mu_l \frac{1}{1 - \Gamma_{T,P}^{1/3}} \dots \dots \dots (4)$$

Mitchell showed that foam behaves approximately as a Bingham plastic fluid in fully developed laminar flow. His shear stress-shear rate relationship for foams with shear rates above 20,000 sec⁻¹ is linear for any quality. The relationship for foam flowing with a shear rate below 20,000 sec⁻¹ can be linearized by subtracting the apparent yield strength. His shear stress-shear rate equation for Bingham Plastic Foam is

$$(\tau - \tau_y) = \mu_p \phi \dots \dots \dots (5)$$

Figure 1 shows Mitchell's plastic viscosity and Figure 2 shows the apparent yield strength. He showed experimentally determined plastic viscosities agree well with Einstein's and Hatschek's theories.

Additional work showed an effective viscosity which combines plastic viscosity and yield point is significantly more reliable than plastic viscosity alone in the determination of Fanning friction factors. The use of effective viscosity of Bingham plastic fluids is technically precise; however, it is interesting to note that most Bingham plastic fluids encountered in the oilfield have small yield strengths compared with their plastic viscosities. Thus, the effective viscosity and the Bingham plastic viscosity are of similar magnitude and are commonly interchanged. However, foam's high yield strength requires the use of effective viscosity.

The effective viscosity in this study is developed with the Hagen-Poiseuille law and the Buckingham-Reiner equation.

The Buckingham-Reiner equation for laminar flow of Bingham plastic fluids within pipes is

$$Q = \frac{\pi \Delta P D^4 g_c}{128 \mu_p L} \left[1 - \frac{4}{3} \frac{\tau_y}{\tau} + \frac{1}{3} \left(\frac{\tau_y}{\tau} \right)^4 \right] \dots \dots \dots (6)$$

The Hagen-Poiseuille law for Newtonian laminar flow within pipes is

$$Q = \frac{\pi \Delta P D^4 g_c}{128 \mu_e L} \dots \dots \dots (7)$$

For the Newtonian turbulent flow relationships to be valid for a Bingham plastic fluid, the flow rate in equation 6 must equal the flow rate in equation 7. A practical solution of this equality shows the effective viscosity of the Bingham plastic foam is

$$\mu_e = \mu_p + \frac{g_c \tau_y D}{6v} \dots \dots \dots (8)$$

Figure 3 illustrates the effective viscosity of foam based on equation 8.

EXPERIMENTAL APPARATUS AND PROCEDURE

Osborne Reynolds' experiments in which streams of dye were injected into water flowing within pipes showed the frictional pressure losses were proportional to average fluid velocity when the dye remained as a stream. This flow regime was called laminar or streamline flow. When mixing of the dye and water occurred the pressure losses were approximately proportional to the square of average fluid velocity. Due to the appearance of the dye mixing with water, the flow regime was called turbulent. Therefore, the flow regimes of a fluid within pipes can be determined by measuring pressure losses and flow rates and comparing their functional relationships.

To generate these functional relationships for foam two horizontal capillary tubes and two horizontal strings of tubing were used in flow tests. The large diameter difference of the tubes and tubing assured any friction loss correlation developed would have wide application. The tubes and tubing also served to produce fully developed laminar and turbulent flow regimes, respectively.

Pressures at each end of either the tubes or tubing, flowing temperature, gas volume, and liquid weight were measured for each flow test. A mass balance, the real gas law, and derived equations were used to calculate foam volumetric flow rate, quality, foam average velocity, shear rate, shear stress, and effective viscosity.

The capillary tubes used were each 24-inches long with internal diameters of 0.0483-inch and 0.0924-inch. The foam for these tests consisted of an aqueous solution of 1% Adofoam BF-1

a commercial anionic surface active agent, and nitrogen. Two calibrated temperature-compensated gauges recorded flowing pressures. The foam was flowed into a plastic separator which was connected to a wet-test meter. The separator was weighed to determine the mass of liquid which was flowed during a test. The effect of quality changes on the foam properties were kept to a minimum by keeping the tubes' discharge pressure above 500 psi. Calculated velocities were less than 20 feet per second. Figure 4 is a diagram of the capillary tube apparatus.

The large diameter tubes were made of eight joints of new J-55 tubing. The 1-1/4-inch 2.40-pound tubing was 194.75 feet long with an internal diameter of 1.380-inch. The 2-3/8-inch, 4.7-pound tubing was 181.32 feet long with an internal diameter of 1.995-inch. An aqueous solution of 1% Dowell F58B, an anionic surface-active agent, was pumped through the tubing strings at rates as high as 7 BPM. Nitrogen was combined with the water at rates to 3000 SCFM. This produced foam volumetric rates to 34.5 BPM. A water storage tank was gauged before and after each test to determine water mass and volume rates. Pump displacements of liquified nitrogen were used to determine nitrogen gas volumetric rate. Pressure losses at the extreme ends of the tubing during the laminar flow tests were measured by a single water manometer inclined at 85° from vertical. Turbulent flow pressure losses were recorded by six differential pressure transducers which were connected across each joint of tubing. Pressures at each end of the tubing strings were measured by two calibrated laboratory gauges. Test pressures to 3000 psi were used. Figures 5 and 6 show the tubing apparatus.

EXPERIMENTAL CORRELATIONS

Mitchell showed that average foam flowing velocity and quality can be accurately determined using a mass balance and the real gas law. The methods used to calculate flowing properties in tubing were only slightly different from the capillary tube. Equations for the capillary tube are presented in the following discussion.

Since the flow tube is in a state of dynamic equilibrium, the mass entering the tube as gas or liquid must leave the tube,

$$M'_{in} = M'_{out} \dots \dots \dots (9)$$

in which

$$M'_{in} = M'_{ll} + M'_{lg} + M'_{gg} + M'_{gl} \dots (10)$$

$$M'_{out} = M'_{lc} - M'_{ld} + M'_{lg} + M'_{wt} + M'_{gl} - M'_{gd} \dots \dots \dots (11)$$

The mass of liquid in the separator is

$$M_{lc} = \frac{g}{g_c} W_{lc} \dots \dots \dots (12)$$

Applying the real gas law and Dalton's law of partial pressures, the mass of gas and water vapor flowing through the wet-test meter is

$$M_{wt} = M_{gm} + M_{lm} = \frac{(P_m - P_v) V_m \bar{M}_g}{z_g R T_g} + \frac{P_v \bar{M}_l V_m}{z_l R T_l} \dots (13)$$

The mass of water vapor and gas displaced from the separator is

$$M_{vs} = M_{gd} = \frac{(P_a - P_v) V_{lc} \bar{M}_g}{z_g R T_g} + \frac{P_v V_{lc} \bar{M}_l}{z_l R T_l} \dots \dots (14)$$

Total measured flowing mass of liquid and gas is thus,

$$M_{lt} = W_l \frac{g}{g_c} + \frac{P_v V_m \bar{M}_l}{z_l R T_l} - \frac{P_v V_{lc} \bar{M}_g}{z_g R T_g} \dots (15)$$

$$M_{gt} = \frac{(P_a - P_v) V_m \bar{M}_g}{z_g R T_g} - \frac{(P_a - P_v) V_{lc} M_g}{z_g R T_g} \dots (16)$$

The volume of gas entering into solution is negligible. Equations 15 and 16 are valid for large diameter tubing if the mass and volume are replaced by mass rate and volumetric rate.

Volumes of saturated gas flowing at the tube pressure and temperature are determined by the perfect gas law. The average pressure of the flow tube can be used only if the differential pressure is small in comparison. Data points with high differential pressure and low average pressure were deleted for the final analysis.

The volume of saturated gas in the tube is

$$V_{sg} = V_{gt} + V_{lv} = \frac{M_{gt} R T_t}{\bar{M}_g (P_t - P_v) z_g} + \frac{V_{gt} P_v}{(P_t - P_v)} \dots (17)$$

The volume of liquid in the tube is

$$V_{lt} = \frac{M_{lt}}{\rho_l} - V_{lv} \dots (18)$$

True foam quality is

$$\Gamma_{T,P} = \frac{V_{sg}}{V_{sg} + V_{lt}} \dots (19)$$

True foam density is

$$\rho_f = \frac{M_{lt} + M_{gt}}{V_{gt} + V_{lt}} \dots (20)$$

Average foam-flowing velocity in the flow tube is

$$v_f = \frac{V_{gt} + V_{lt}}{4 t D^2} \dots (21)$$

The effective foam viscosity, true density and pipe diameter, and average foam velocity is used to calculate shear stress at the wall of the pipe, average shear rate, Reynolds number, and Fanning friction factor.

Average shear rate and shear rate at the wall of the tube for a Bingham plastic fluid is

$$\phi_a = \phi_w = \frac{8v}{D} \dots (22)$$

Shear stress at the wall is

$$\tau_w = \frac{D \Delta P}{4L} - \tau_y \dots (23)$$

The Reynolds number and Fanning friction factor are

$$N_R = \frac{v_f D \rho_f}{\mu_e} \dots (24)$$

$$f = \frac{\Delta P D}{L \rho_f v_f^2} \dots (25)$$

Plots of the shear stress-shear rate relationships are given in Figures 7 through 9. Foams of constant quality show two distinct flow regimes. Below critical shear rates for each pipe diameter and foam quality the slope of the shear stress-shear rate function is 1.0, indicating laminar Bingham plastic flow. Above this critical shear rate the slope is approximately 2.0 and the foam is in turbulent flow. Calculated slopes of the turbulent shear stress-shear rate relationship are between 1.86 and 2.01.

The critical shear rate for foams corresponds with a critical Reynolds number between 2000 and 2500. Figure 10 is a conventional single-phase fluid Moody diagram with the foam data superimposed. The algebraic standard deviation of friction factors calculated with this data compared with the Colebrook method normally used for single-phase fluids is 0.05 for the laminar flow regime and 0.188 for the turbulent flow regime.

APPLICATION OF METHOD FOR PREDICTION OF FRICTIONAL LOSSES IN PIPES

EXAMPLE CALCULATIONS

1. Laminar Flow

Determine the pressure-loss gradient of 0.80 quality foam flowing within a 1.00-inch diameter pipe at 1.0 BPM.

1. a. Average foam velocity,
 $v_f = 17.16$ fps
- b. From equation 8, effective viscosity, $\mu_e = 29$ cps
- c. Foam density may be approximated by neglecting gas in solution and the vapor pressure of water.
Approximate foam density,
 $\rho_f = \rho_l(1-\Gamma) = 1.67$ ppg
- d. From equation 24, Reynolds number, $N_R = 917$ $N_R < 2000$, therefore, flow is laminar.
- e. From equation 6, laminar pressure-loss gradient,
 $\frac{\Delta P}{\Delta L} = 0.590$ psi/ft.

2. Turbulent Flow

Determine pressure-loss gradient for the laminar flow example with a flow rate of 5.0 BPM.

- a. Average foam velocity,
 $v_f = 85.8$ fps
- b. Effective foam viscosity,
 $\mu_e = 10.9$ cps
- c. Approximate foam density,
 $\rho_f = 1.67$ ppg
- d. Reynolds number, $N_R = 1.21 \times 10^4$
 $N_R < 2000$ Therefore, flow is turbulent
- e. From Figure 12 Fanning friction factor, $f = .0075$
- f. From equation 25, turbulent pressure-loss gradient,
 $\frac{\Delta P}{\Delta L} = 3.57$ psi/ft

FIELD APPLICATION

Wellhead pressure during a fracture treatment using foam flowing at 14 BPM in 2-7/8-inch tubing at 7000 feet was predicted using the proposed method. The total calculated wellhead pressure was 5250 psi and measured pressure was 5350 psi.

Other wells have been fractured through 4-1/2-inch and 5-1/2-inch casing and the calculated wellhead pressures have been within 2% of the actual pressures during treatment.

CONCLUSIONS

1. Foam behaves as a single-phase Bingham plastic fluid.
2. Effective viscosity of foam must be used for calculating pressure losses for flowing foam.
3. Friction losses for foam may be determined as for a single-phase fluid using conventional Reynolds number and Moody diagram.
4. Friction losses in oilfield pipes can be accurately predicted for any combination of foam flow rate and pipe size.

NOMENCLATURE

- D = inside diameter of tube, in
 f = Fanning friction factor
 g_c = gravitational constant, 32.2
 L = tube length, ft
 M = mass at atmospheric conditions, Lbm
 M' = mass at flowing conditions, Lbm
 \bar{M} = molecular weight
 N_R = Reynolds number
 P = pressure, psia
 ΔP = pressure drop between ends of tube, psid
 Q = foam quality
 R = universal gas constant,
 $10.732 \frac{(PSIA)(FT^3)}{(Lb-mole)(^\circ R)}$
 T = temperature, $^\circ R$
 t = time, sec
 V = volume, ft^3
 v = velocity, ft/sec

w = weight, Lbf
z = compressibility factor

SUBSCRIPTS

a = average tube
e = effective
f = foam
g = gaseous phase
gd = gas displaced from separator
gg = gas-phase in gaseous state
gl = gas-phase absorbed into the liquid phase
gm = saturated gas measured by wet-test meter
gt = gas flowing in tube
in = entering tube
l = liquid
lc = liquid in the separator
ld = liquid-phase vapor displaced from separator
lg = liquid-phase in gaseous state
ll = liquid-phase in liquid state
lm = liquid-phase vapor measured by wet-test meter
lt = liquid at flowing conditions
m = wet-test meter
out = existing tube
P = Bingham plastic
sg = saturated gas
t = tube
v = vapor
vs = saturated gas displaced from separator
w = wall

GREEK SYMBOLS

$\Gamma_{T,P}$ = foam quality at specified temperature and pressure
 ϕ = shear rate, sec^{-1}
 ρ_f = true foam density, Lbm/ft^3
 τ = shear stress, Lbf/ft^2
 τ_y = yield strength, Lbf/ft^2
 μ = viscosity, cP

ACKNOWLEDGEMENTS

The authors wish to thank Dowell and NOWSCO for their assistance in the tubing tests.

REFERENCES

1. Lockhart, R. W. and Martinelli, R. C.: "Proposed Correlations of Data for Isothermal Two-Phase, Two Component Flow in Pipes," Chem. Eng. Progr., 1949, v. 45, p. 39.
2. Baker, O.: "Experiences with Two-Phase Pipelines," paper presented before the joint meeting of Canadian Natural Gas Processing Assn. and the Natural Gasoline Assn. of America, Calgary, Alberta, Sept. 15 1960.
3. Dukler, A. E., et al: "Frictional Pressure Drop in Two-Phase Flow: B-An Approach Through Similarity Analysis", AICHE J., 1964, v. 10, p. 44-51.
4. Hughmark, G. A.: "Hold-Up In Gas-Liquid Flow", Chem. Eng. Progr., 1962, v. 58, p. 62-65.
5. Eaton, Ben A., et al: "The Prediction of Flow Patterns, Liquid Hold-Up and Pressure Losses Occurring During Continuous Two-Phase Flow in Horizontal Pipelines", J. Petrol. Technol., June 1967, p. 315-328.
6. Bertuzzi, A. F., Tek, M. R., and Poettmann, F. H.: "Simultaneous Flow of Liquid and Gas Through Horizontal Pipe," Trans. AIME, 1956, v. 207, p. 17-24.

- | | |
|--|---|
| <p>7. Einstein, Albert: "Eine Neve Bestimmung Der Molekuldimensionen", <u>Annalen Der Physik</u>, 1906, v. 19, SFR 4, p. 289.</p> <p>8. Hatschek, Emil: "Die Viskositat Der Dispersoide. I. Suspensoide," <u>Kolloid Z.</u>, 1910, v. 7, p. 301-304.</p> <p>9. _____: "Die Viskositat Der Dispersoide. II Die Emulsionen Uno Emulsoide," <u>Kolloid Z.</u>, 1910, v 8, p. 34-39.</p> | <p>10. Mitchell, B. J.: <u>Viscosity of Foam</u>, Ph.D. thesis, Univ. Okla., 1969.</p> <p>11. _____: "Test Data Fill Theory Gap on Using Foam as a Drilling Fluid," <u>Oil and Gas J.</u>, Sept. 6, 1971, p. 96-100.</p> <p>12. Krug, J., Mitchell, B. J.: "Charts Help Find Volume, Pressure Needed for Foam Drilling", <u>Oil and Gas J.</u>, Feb. 7, 1972, p. 61-64.</p> |
|--|---|

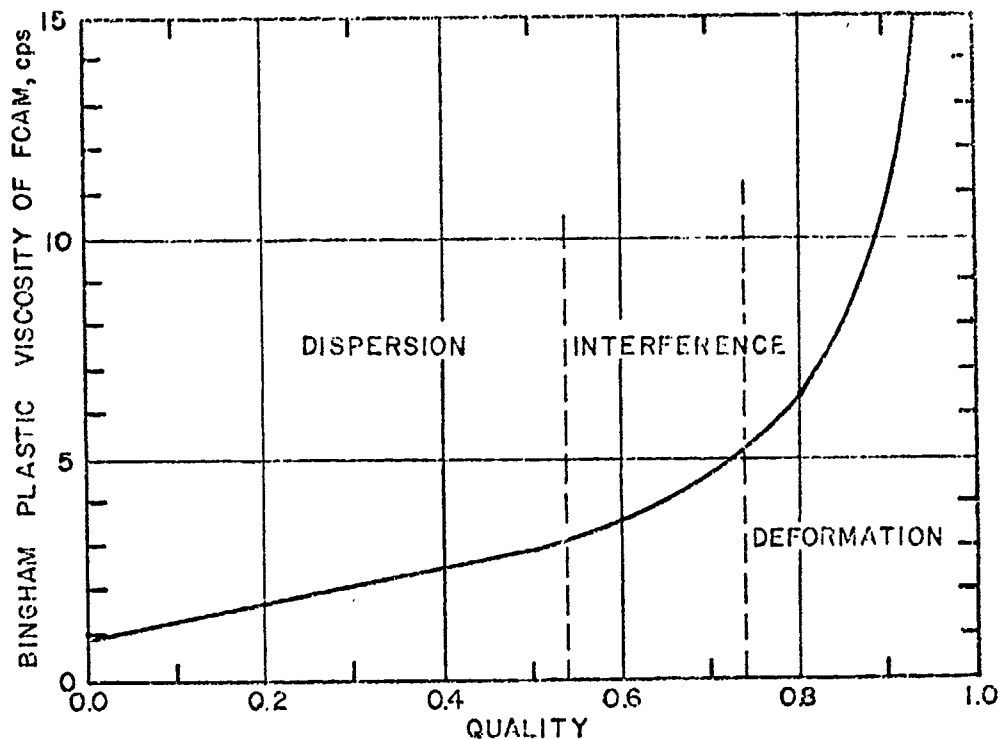


Fig. 1 - Bingham plastic viscosity of foam.

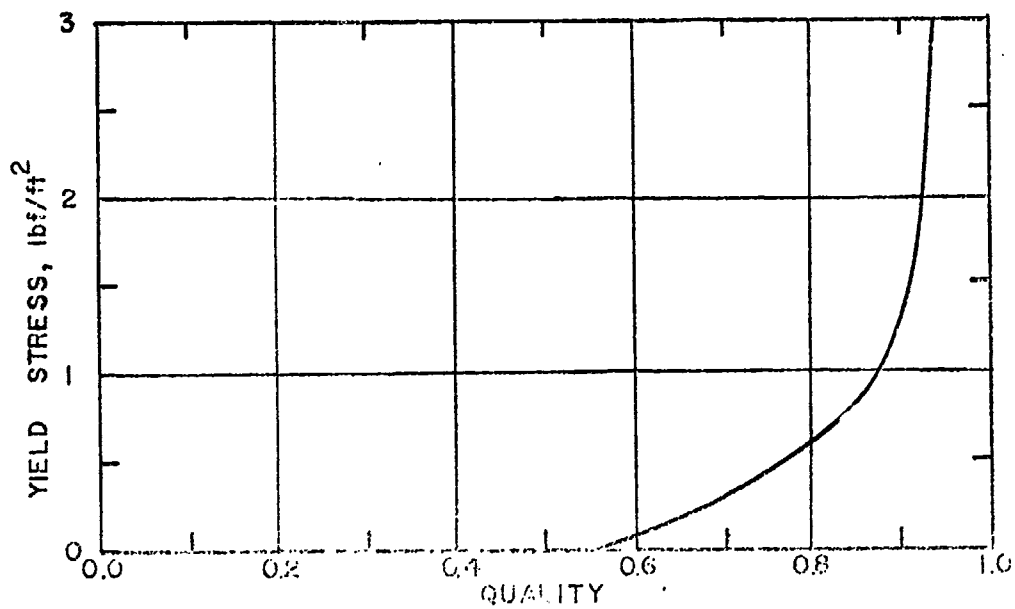


Fig. 2 - Yield stress of foam.

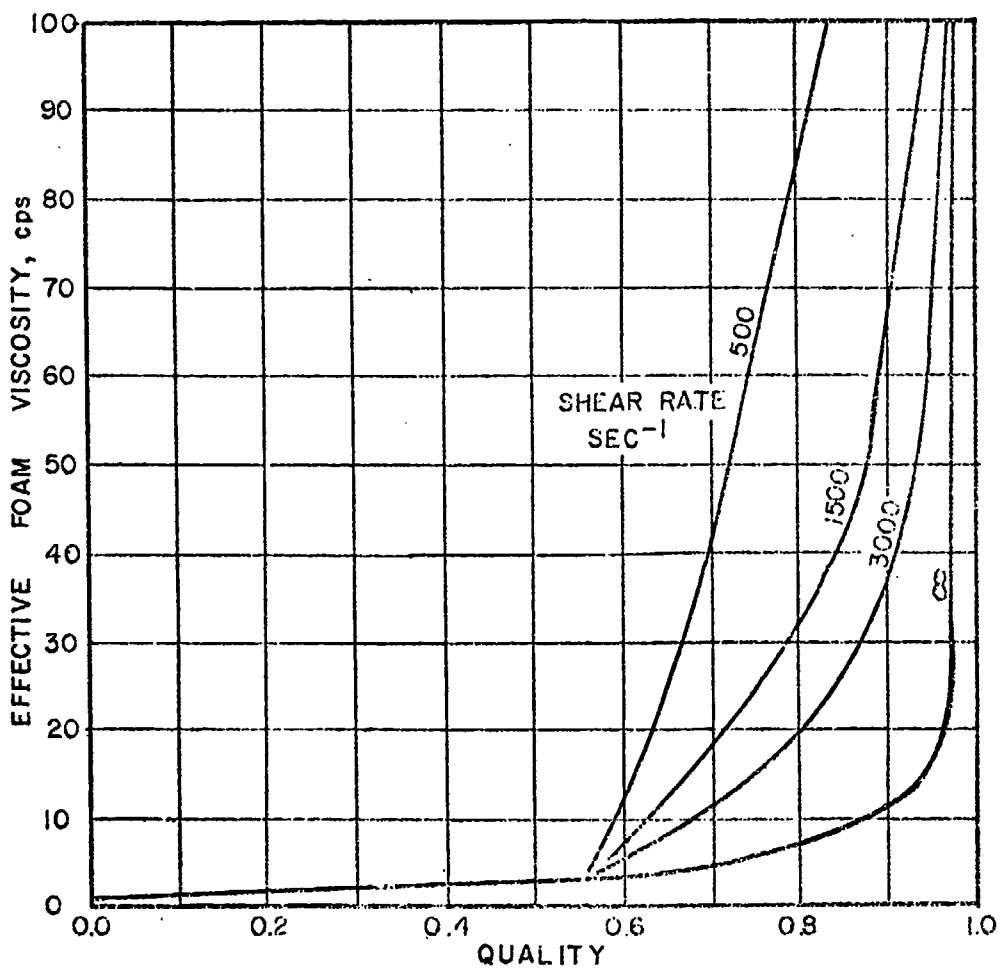


Fig. 3 - Effective viscosity of foam.

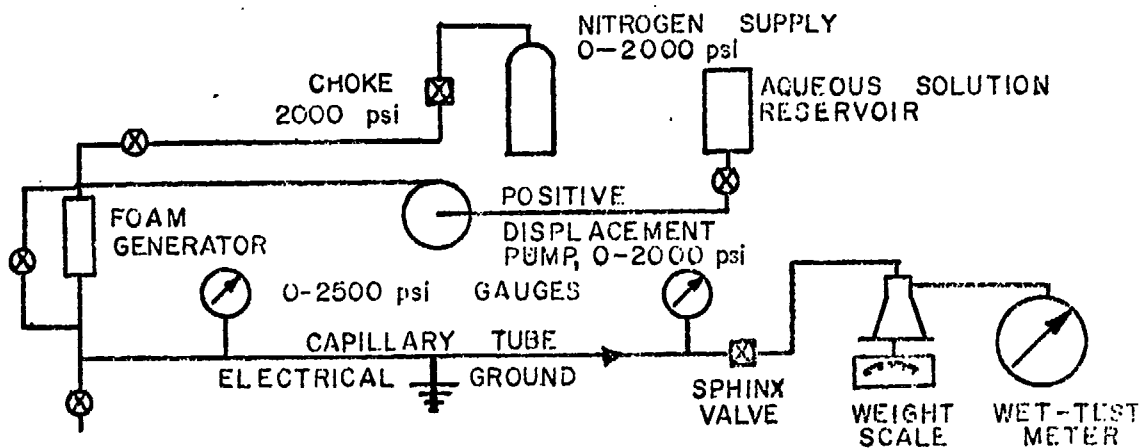


Fig. 4 - Capillary tube apparatus.

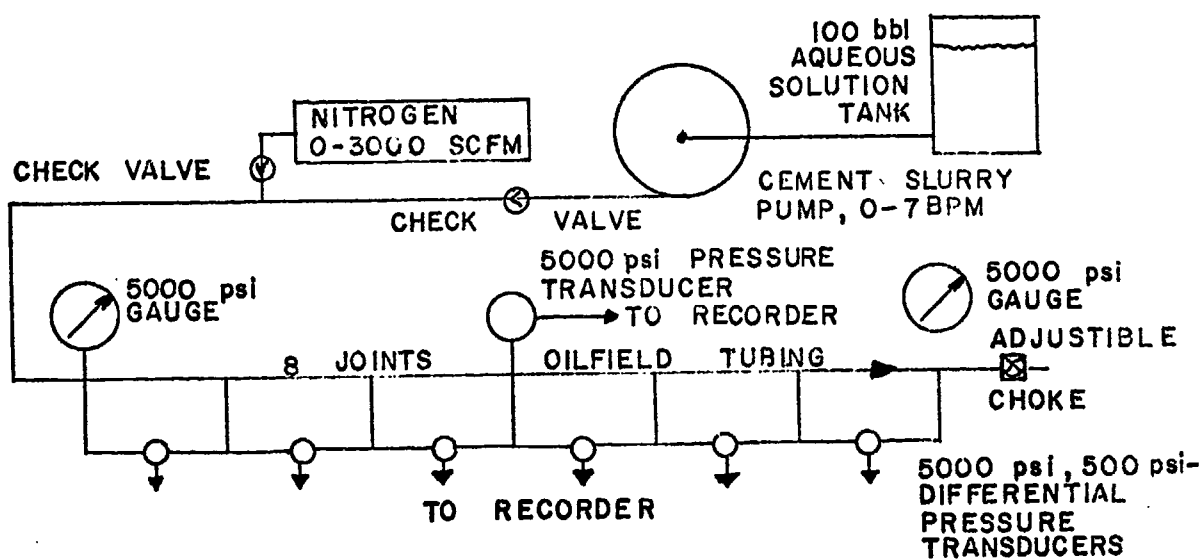


Fig. 5 - Turbulent flow regime tubing apparatus.

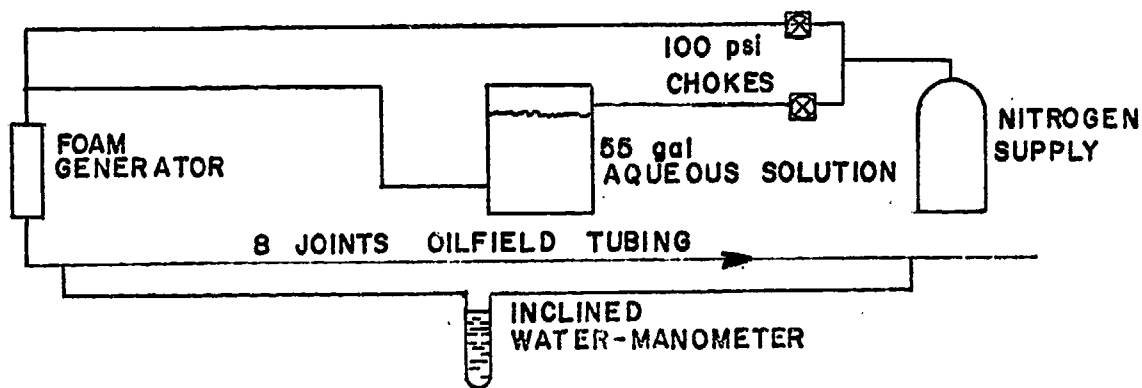


Fig. 6 - Laminar flow regime tubing apparatus.

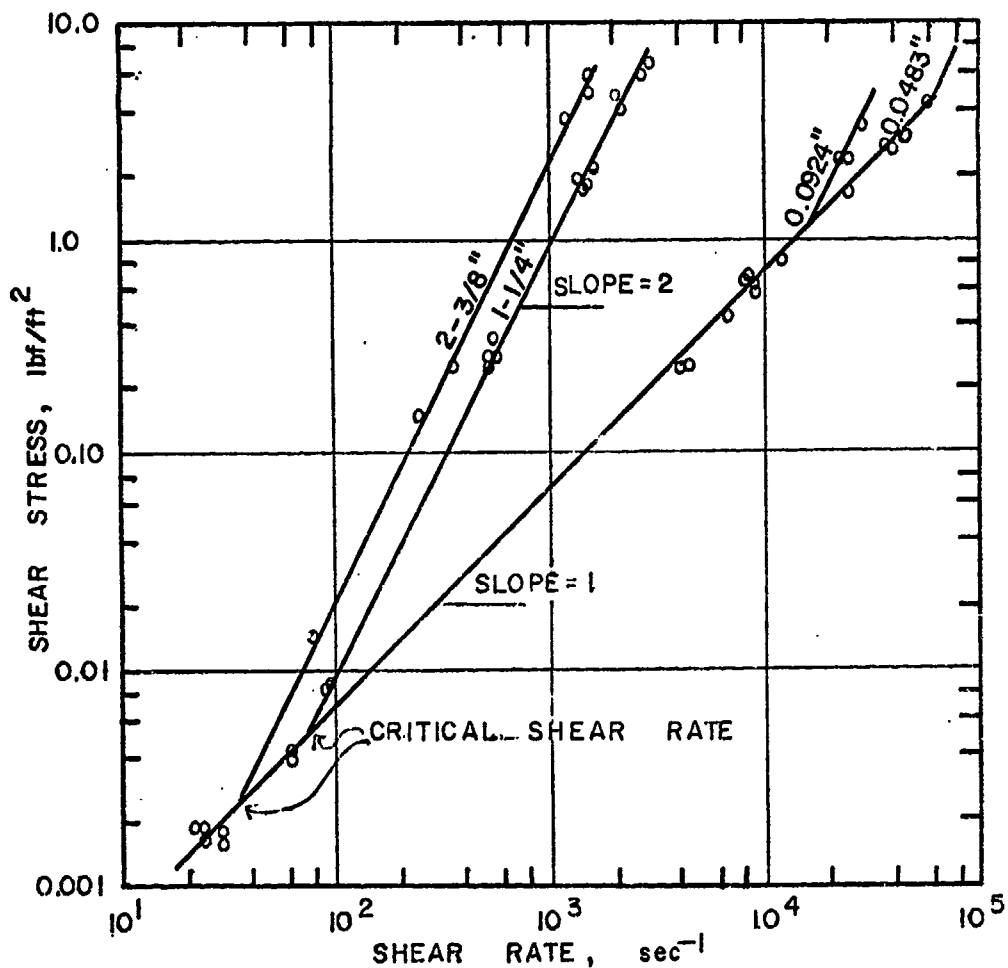


Fig. 7 - Shear stress-shear rate relationship for 0.50 quality foam.

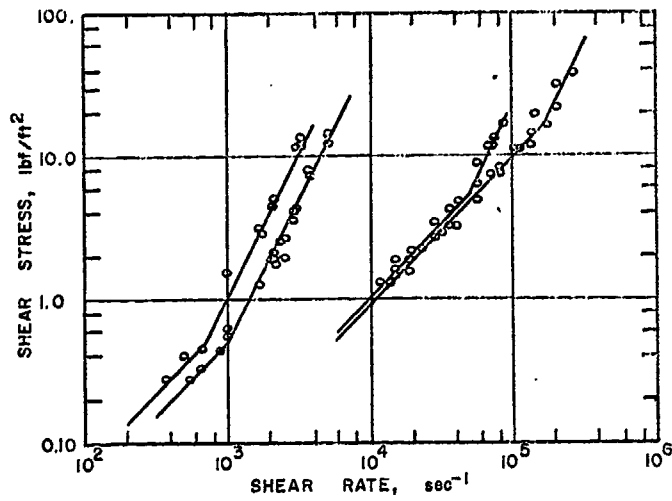


Fig. 8 - Shear stress-shear rate relationship for 0.70 quality foam.

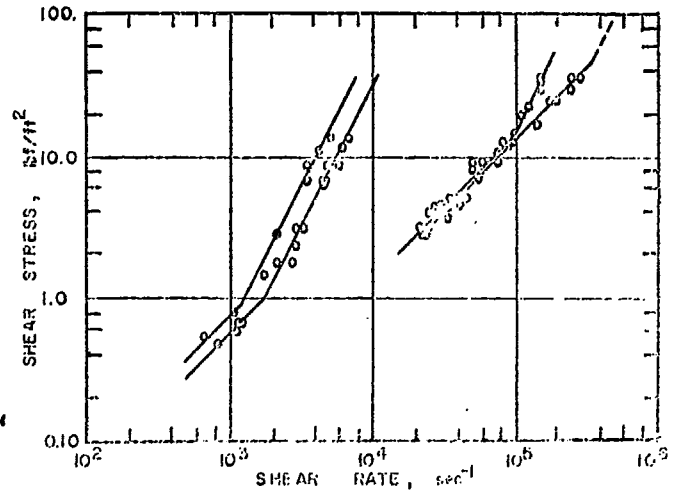


Fig. 9 - Shear stress-shear rate relationship for 0.80 quality foam.

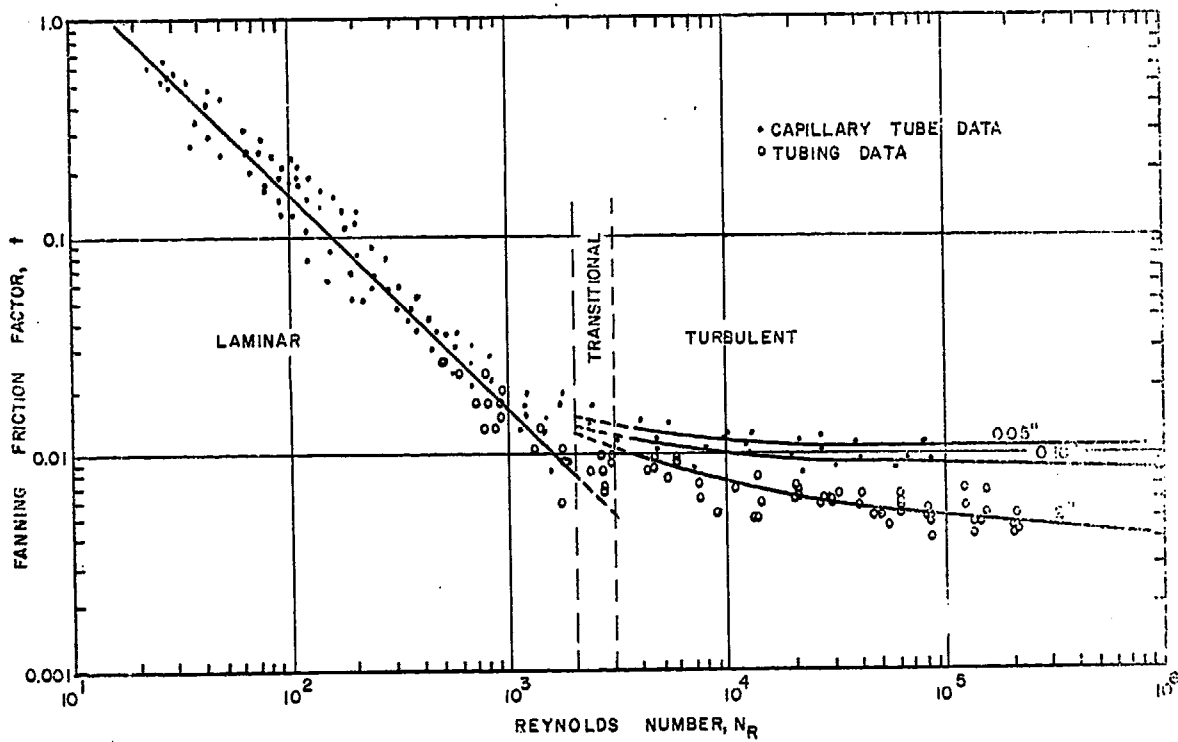


Fig. 10 - Moody diagram for foam.